Received: 30 September 2019 | Revised: 28 July 2020 | Accepted: 6 August 2020

DOI: 10.1002/cne.25003

RESEARCH ARTICLE

JCN RESEARCH IN SYSTEMS NEUROSCIENCE THE JOURNAL OF COMPARATIVE NEUROLOGY WILEY

Ontogeny of the electric organ discharge and of the papillae of the electrocytes in the weakly electric fish *Campylomormyrus rhynchophorus* (Teleostei: Mormyridae)

Yevheniia Korniienko[1] | Ralph Tiedemann[2] | Marianne Vater[3] | Frank Kirschbaum[1]

[1]Humboldt University of Berlin, Faculty of Life Sciences, Albrecht Daniel Thaer-Institute of Agricultural and Horticultural Sciences, Unit of Biology and Ecology of Fishes, Berlin, Germany

[2]University of Potsdam, Institute of Biochemistry and Biology, Unit of Evolutionary Biology / Systematic Zoology, Potsdam-Golm, Germany

[3]Unit of General Zoology, Institute of Biochemistry and Biology, University of Potsdam, Potsdam Golm, Germany

Correspondence
Frank Kirschbaum, Humboldt University of Berlin, Faculty of Life Sciences, Albrecht Daniel Thaer-Institute of Agricultural and Horticultural Sciences, Unit of Biology and Ecology of Fishes, Philippstr. 13, House 16, D-10115 Berlin, Germany.
Email: frank.kirschbaum@staff.hu-berlin.de

Funding information
Friedrich Naumann Foundation for Freedom in the course of a scholarship for international PhD students; Friedrich Naumann Stiftung, Grant/Award Number: Grant for international students

Abstract

The electric organ of the mormyrid weakly electric fish, *Campylomormyrus rhynchophorus* (Boulenger, 1898), undergoes changes in both the electric organ discharge (EOD) and the light and electron microscopic morphology as the fish mature from the juvenile to the adult form. Of particular interest was the appearance of papillae, surface specializations of the uninnervated anterior face of the electrocyte, which have been hypothesized to increase the duration of the EOD. In a 24.5 mm long juvenile the adult electric organ (EO) was not yet functional, and the electrocytes lacked papillae. A 40 mm long juvenile, which produced a short biphasic EOD of 1.3 ms duration, shows small papillae (average area 136 μm^2). In contrast, the EOD of a 79 mm long juvenile was triphasic. The large increase in duration of the EOD to 23.2 ms was accompanied by a small change in size of the papillae (average area 159 μm^2). Similarly, a 150 mm long adult produced a triphasic EOD of comparable duration to the younger stage (24.7 ms) but featured a prominent increase in size of the papillae (average area 402 μm^2). Thus, there was no linear correlation between EOD duration and papillary size. The most prominent ultrastructural change was at the level of the myofilaments, which regularly extended into the papillae, only in the oldest specimen—probably serving a supporting function. Physiological mechanisms, like gene expression levels, as demonstrated in some *Campylomormyrus* species, might be more important concerning the duration of the EOD.

KEYWORDS

Campylomormyrus, electric organ discharge, electrocyte ontogeny, electrocyte ultrastructure, papillae

1 | INTRODUCTION

Electric organs (EOs) are composed of action-potential generating cells, the electrocytes, whose summed activity produces an electrical pulse, the electric organ discharge (EOD). The EOs have evolved in cartilaginous and teleostean fishes eight times due to convergent evolution (Bass, 1986a, 1986b; Bullock & Heiligenberg, 1986; Kirschbaum, 2020; Moller, 1995). The most speciose groups are the South American knifefish (Gymnotiformes) (Crampton, 2006; Crampton, Rodriguez-Cuttaneo, Lovejoy, & Caputi, 2013) with ~250 species and the African mormyrids comprising more than 200 species (Sullivan, Lavoué, & Hopkins, 2016).

[Correction added on 19 September 2020, after first online publication: Projekt Deal funding statement has been added.]

The weakly electric mormyrids possess a larval EO (Kirschbaum, 1977, 1981) early during ontogeny and an adult EO that persists in adults (Westby & Kirschbaum, 1978). In addition to the EOs, the mormyrids possess electroreceptors (Bullock & Heiligenberg, 1986; Bullock, Hopkins, Popper, & Fay, 2005; Szabo, 1974; Webb et al., 2020), which sense the fish's own electric field and that of other weakly electric fish. Thus, this sensory system enables these fish to electrolocate (orientation) (von der Emde, 1992, 1999, 2006) and to electrocommunicate (e.g., Kramer, 1990; Moller, 1995; Worm, Kirschbaum, & von der Emde, 2017).

The mormyrid adult EO is composed of four colums of electrocytes, two dorsal and two ventral ones (Figure 1f). In each column between 21 and 91 disc-shaped electrocytes (number depending on species, Bass, 1986a) are arranged in parallel (Figure 1e–g). The individual electrocytes are grouped in a 90° angle along the longitudinal axis of the fish (Figure 1f). They are derivatives of myotomes as evidenced by a central zone of myofibrils and possess several unique specializations (Bass, Denizot, & Marchaterre, 1986; Denizot, Kirschbaum, Westby, & Tsuji, 1978; Denizot, Kirschbaum, Westby, & Tsuji, 1982; Szabo, 1960). Each electrocyte forms multiple finger-like processes, the stalks, which join together to a larger stalk, which receives the innervation by spinal electromotor neurons (Szabo, 1958). The stalks arise either at the posterior or the anterior face of the electrocyte. In some species the stalks penetrate the central axis of the electrocyte (Bass, 1986a, 1986b). Each stalk and face of an electrocyte generates an action potential and the summed activity determines the shape of the EOD (Bennett & Grundfest, 1961). Thus different geometries of the mormyrid electrocytes lead to different EOD types concerning polarity and number of phases (Bass, 1986b). The duration of the EOD, however, was correlated with specializations of the electrocyte's anterior face such as the degree of surface proliferations in the form of tubule-like structures (tubules) and calveoli (Bass et al., 1986; Luft, 1958), which are more pronounced in species with longer EODs (Bass et al., 1986). The increased electrocyte's surface leads to a longer EOD presumably by increasing the membrane capacitance (Bennett, 1970).

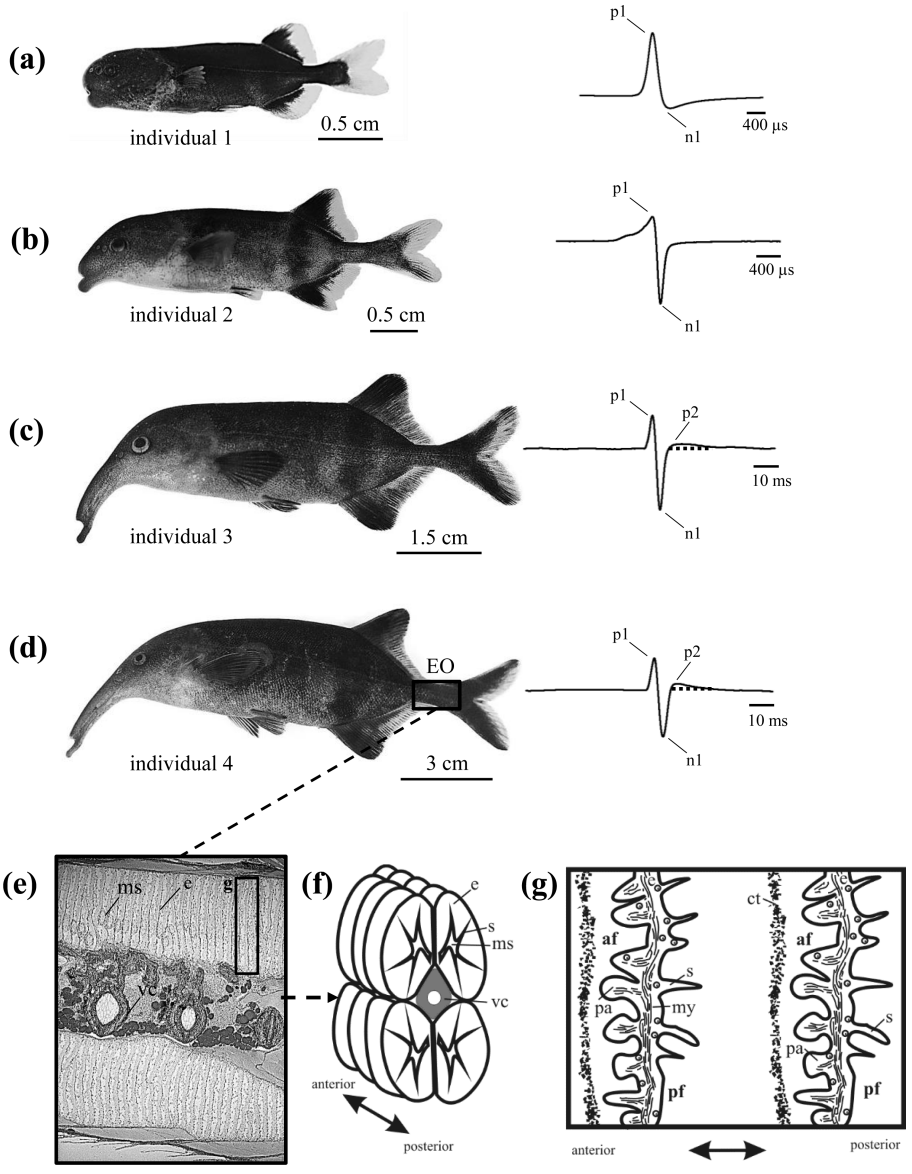

FIGURE 1 Morphology of four developmental stages of *Campylomormyrus rhynchophorus* (left) (a–d) and the corresponding representative EOD (right). Amplitude values of the EOD are scaled to the same peak-to-peak amplitude. The different phases of the EOD are denoted as p1, first head positive phase; p2 second head positive phase; and n1, first head negative phase. Note differences in time scales. The EOD of the 24.5 mm long specimen (a) represents the activity of the larval EO (for details see text). The EODs of the three larger specimens are the activity of the adult EO. Note the change in the duration of the EOD, in particular between the 40 (b) and 79 mm long specimen (c). A medial sagittal section (e) through the dorsal and ventral columns (vc) of the EO of one side, shows the many individual electrocytes (e) with their main stalks (ms) arranged in parallel in the longitudinal axis of the fish. In f the organization of the EO is shown schematically in oblique view. In figure g two electrocytes are shown schematically in sagittal section with their main structures: stalks (s) at the posterior face (pf), papillae (pa) at the anterior face (af), centrally located myofibrils (my) and the connective tissue (ct)

In the mormyrid genus *Campylomormyrus* there are species with very short EODs (ca. 200 μs duration) (e.g., *C. compressirostris* [Pellegrin, 1924]) and others with very long EODs (ca. 25 ms duration) (Feulner, Kirschbaum, Mamonekene, Ketmaier, & Tiedemann, 2007; Feulner, Kirschbaum, & Tiedemann, 2008; Lamanna, Kirschbaum, & Tiedemann, 2016). In species with the longest EODs of about 25 ms duration, as in *C. numenius* (Boulenger, 1898) (Paul et al., 2015) and *C. rhynchophorus* (Boulenger, 1898) (Nguyen et al., 2020), there are additional large foldings or evaginations on the anterior face of the electrocyte, so called papillae, which increase the surface area of the electrocyte even further. In one of the few ontogenetic studies of weakly electric fish, it was shown that *C. rhynchophorus* produces a short juvenile EOD which elongates by a factor of about 25 during ontogeny, a process which is accompanied by a proliferation of papillae on the anterior face of the electrocytes (Nguyen et al., 2020). Since *C. rhynchophorus* can be bred in captivity (Nguyen et al., 2017), we choose this species for a longitudinal study of the EOD development and a detailed study of the fine structure of the papillae in order to find out, if there is indeed a correlation between the duration of the EOD and the size increase of the papillae.

2 | MATERIALS AND METHODS

2.1 | Fish

For reproduction, we used a pair (male of 37 cm, female of 31 cm total length) of *C. rhynchophorus*, which was originally purchased via a wholesale-dealer in Germany from the African region around Brazzaville from the Congo River. These fish were identified as to their systematic position by genetic analysis (Feulner et al., 2008). They were kept in tap water (temperature between 25 and 28°C, water conductivity 660 μS/cm, pH 7.4). Decrease of conductivity for several weeks down to 224 μS/cm (this led to a pH decrease to 6.5 as well) induced ripening of the gonads (see Nguyen et al., 2017). The ripe fish were injected with gonadotropin-releasing hormone (commercial name Ovaprim: GnRH + Domperidone; Western Chemical Inc., Ferndale, WA 98248) to induce ovulation, to enhance sperm release, and to perform artificial reproduction. One hundered and sixty-two eggs were obtained of which 62 hatched.

2.2 | Rearing

Eggs, free embryos and larvae were kept in plastic petri dishes (⌀ = 8.6 cm, h = 1.5 cm) for about 40 days. Freshly hatched *Artemia nauplii* were offered twice a day and up to a size of about 40 mm, the juveniles were in addition fed small (ca. 2–4 mm) live chironomid larvae. Afterwards, the fish were transferred to small glass tanks (30 x 20 x 20 cm) with a density of about 15–20 larvae per tank. Larger fish were fed as the adults; the adult fish were fed twice daily with live *Chaoborus* (*Corethra*) and chironomid larvae or frozen larvae.

2.3 | Photography

The morphology of the fish was documented with a digital camera Canon EOS 350D and Canon EOS 100D in anesthetized specimens.

2.4 | Oscilloscope recordings

The EODs were recorded by using a Tektronix TDS 3012B digital phosphor oscilloscope (maximum sampling rate: 1.25 GS/s; 9 bit vertical resolution). For larvae with a size of 24.5 mm, we used a Tektronix ADA 400A differential preamplifier (variable gain; 0.1x, 1x, 10x, 100x and bandwidth 100 Hz–1 MHz) and a Tektronix TM 502A differential amplifier (upper bandwidth 3 kHz)—for juvenile and adult fish. All EOD-recordings were made in water of a temperature of 25–26 ± 0.5°C and the water conductivity was of about 600–700 μS/cm. The EOD of the fish was recorded in plastic aquaria of different sizes: the recording tank measured 11 × 11 mm for the larvae, 7 × 5 cm for the small juveniles, and 13 × 15 cm for the largest fish. The water level was adjusted according to the size of the fish. The positive electrode was placed near the head of the fish and the negative near the tail. These different recording conditions led to amplitude values, which were not comparable between different size groups of fish (see e.g., Table 1).

2.5 | Histological and microscopical techniques

Four specimens (24.5; 40; 79 and 150 mm in total length; individuals 1–4) were euthanized with an overdose of tricaine methanesulfonate (MS-222) prior to fixation. The tail and the caudal peduncle were cut off and fixed by immersion for 24 hr in 1% paraformaldehyde and 2.5% glutaraldehyd in 0.1 M phosphate buffer. For the semi-thin sections, tissues were post-fixed in 1% osmium tetroxide for an additional 1–2 hr and then washed twice with 0.1 M phosphate buffer for half an hour. Then, the tissues were dehydrated in a graded alcohol series from 50 to 100% (30 min each, two changes). Following this, tissues were placed in propylenoxid for 30 min (twice) and then kept in a 50: 50 mixture of epoxy resin (Durcupan, Electron Microscopy Sciences) and propylenoxid for 1 hr and 70:30 overnight. The tissue was then embedded in beam cups containing

TABLE 1 Durations (D) of the different phases (p1, p2, n1; see Figure 1) of the EOD during development

Specimen	Size (TL) mm	D (p1) ms	D (p2) ms	D (n1) ms	TD ms
Indiv. 2	40	0.6	-	0.7	1.3
Indiv. 3	79	3.9	13.9	5.4	23.2
Indiv. 4	150	4.3	15.2	5.2	24.7

Abbreviations: TD, total duration of EOD; TL, total length of the fish.

100% Durcupan and polymerized for 1 day at 40°C and for 2 days at 60°C (method described by Robinson et al., 1985). After trimming, serial sagittal sections, 1 μm thick, were prepared using an ultramicrotome. The sections were mounted on glass slides and stained with Richardson blue.

The semi-thin sections were studied by light microscopy using a Leica microscope DM4000B to determine the right areas for future ultra-thin sectioning. Ultra-thin sections, of about 70 nm, were cut with a diamond knife on the ultramicrotome in the sagittal plane; about 10 sections per specimen were cut. After cutting, the ultra-thin sections were collected on single slot grids coated with Formvar (Electron Microscopy Sciences) from the distilled water surface. Remaining water was absorbed with filter paper. Finally, the ultra-thin sections were contrasted with uranyl acetate (1%) and lead acetate. The micrographs were obtained on a transmission electron microscope (JEM 1011, manufacturer JEOL).

2.6 | Determination of the size of the papillae

For the determination of the number and size of the papillae, we choose a 200 μm long stretch of three different electrocytes in the three specimens—number 2 (40 mm total length), 3 (79 mm total length) and 4 (150 mm total length), respectively. The length of the papillae was measured from the central alignment of the myofibrils on and the width was determined as the maximum width of the papillae. From these values, the area of the papillae was calculated.

3 | RESULTS

3.1 | Ontogeny of morphology and EOD

A juvenile of 24.5 mm total length (Figure 1a) lacks the uniform black pigmentation in the unpaired fins and the elongated snout typical of adult *C. rhynchophorus*. The EOD is a biphasic discharge with a large head positive peak (p1) and a short head negative phase (n1) (Figure 1a) of about 1 ms total duration. This is a typical EOD of the larval EO (Werneyer & Kramer, 2006; Westby & Kirschbaum, 1977) that is located in the deep lateral muscle (Kirschbaum, 1981). The treatment of the larval EO is beyond the scope of the present article. At this 24.5 mm stage, the adult EO, that is located in the caudal peduncle, is not yet functional. In a 40 mm long juvenile (Figure 1b) the elongation of the snout has started and the unpaired fins are now completely black. The EOD is biphasic and composed of a short head positive and a long head negative phase (Figure 1b) with a total duration of about 640 μs. This juvenile EOD is the first activity of the adult EO (Kirschbaum et al., 2016; Nguyen et al., 2017, 2020). The transition from the larval to the juvenile EOD (see Nguyen et al., 2020) is not shown here, because the treatment of the larval EO is beyond the scope of the present article. At 79 mm total length the juvenile possesses a long snout (Figure 1c) and has a slightly larger body height than the younger stages. The EOD has now changed into a triphasic discharge (Figure 1c) due to the addition of a long, second head positive phase (p2). Total EOD duration amounts to about 25 ms. The 150 mm fish is at the start of adulthood, the snout is slightly longer than in the 79 mm juvenile, the body height has further increased. The EOD (Figure 1d) is nearly identical to that of the 79 mm juvenile. Figure 1e shows a sagittal section through the dorsal and ventral columns of the adult EO of the 24.5 mm long fish. The typical arrangement of the mormyrid adult EO is present with many individual electrocytes arranged in the longitudinal axis of the fish. The schematic oblique 3D view of the two dorsal and ventral columns of electrocytes illustrates the caudal location of the stalk system (Figure 1f). Figure 1g shows a scheme of two electrocytes of the largest specimen in sagittal section, with their central band of myofibrils, the anterior evaginations, the papillae, and the posterior evaginations, the stalks. Each electrocyte is enclosed in a sheath of loose connective tissue.

3.2 | Ontogeny of the electrocytes at the light microscopical level

Figure 2 compares sagittal sections of the electrocytes in four developmental stages at the light microscopical level. Electrocytes are separated by connective tissue, in all developmental stages, and contain numerous nuclei within both the anterior and posterior faces. In the electrocytes of the 24.5 mm fish (Figure 2a), in which only the larval EO is active, a few small stalks originate from the posterior face. Papillae are not yet present and myofibrils are not clearly delineated in the light microscopical view. In the 40 mm long specimen, that produces a short juvenile EOD (Figure 2b; note that the EOD is shown at two different time scales), papillae have started to develop along the anterior face between 10 and 20 μm long. The stalks of the posterior face are more numerous now than before. Myofibrils are distinct in the central area of the electrocyte. In the 79 mm long juvenile (Figure 2c) papillae have increased in size (ca. 15–25 μm long) and stalks are frequent. In the 150 mm long specimen (Figure 2d) the papillae have considerably increased in size (ca. 70–80 μm long) and the myofibrils regularly extend deep into the longest papillae.

3.3 | EOD characteristics and number and area of the papillae at three ontogenetic stages

We investigated structural-functional correlations by comparing the EOD duration with morphological features of the papillae. There is a prominent increase in the total duration of the EOD from the 40 to the 79 mm long fish (from 1.3 to 23.2 ms) but only a slight increase in duration from the 79 to the 150 mm long juvenile (from 23.2 to 24.7 ms) (Table 1, Figure 3). The number of papillae per 200 μm long stretch varies between 19 and 21 in the 40 mm long fish, between 17 and 19 in the 79 mm long fish and between 14 and 16 in the 150 mm long fish. The size of the papillae expressed as their area increases slightly from 136 μm^2 in the 40 mm fish to 159 μm^2 in the 79 mm fish, and more than doubles to a value of 402 μm^2 in the 150 mm fish. (Table 2, Figure 3).

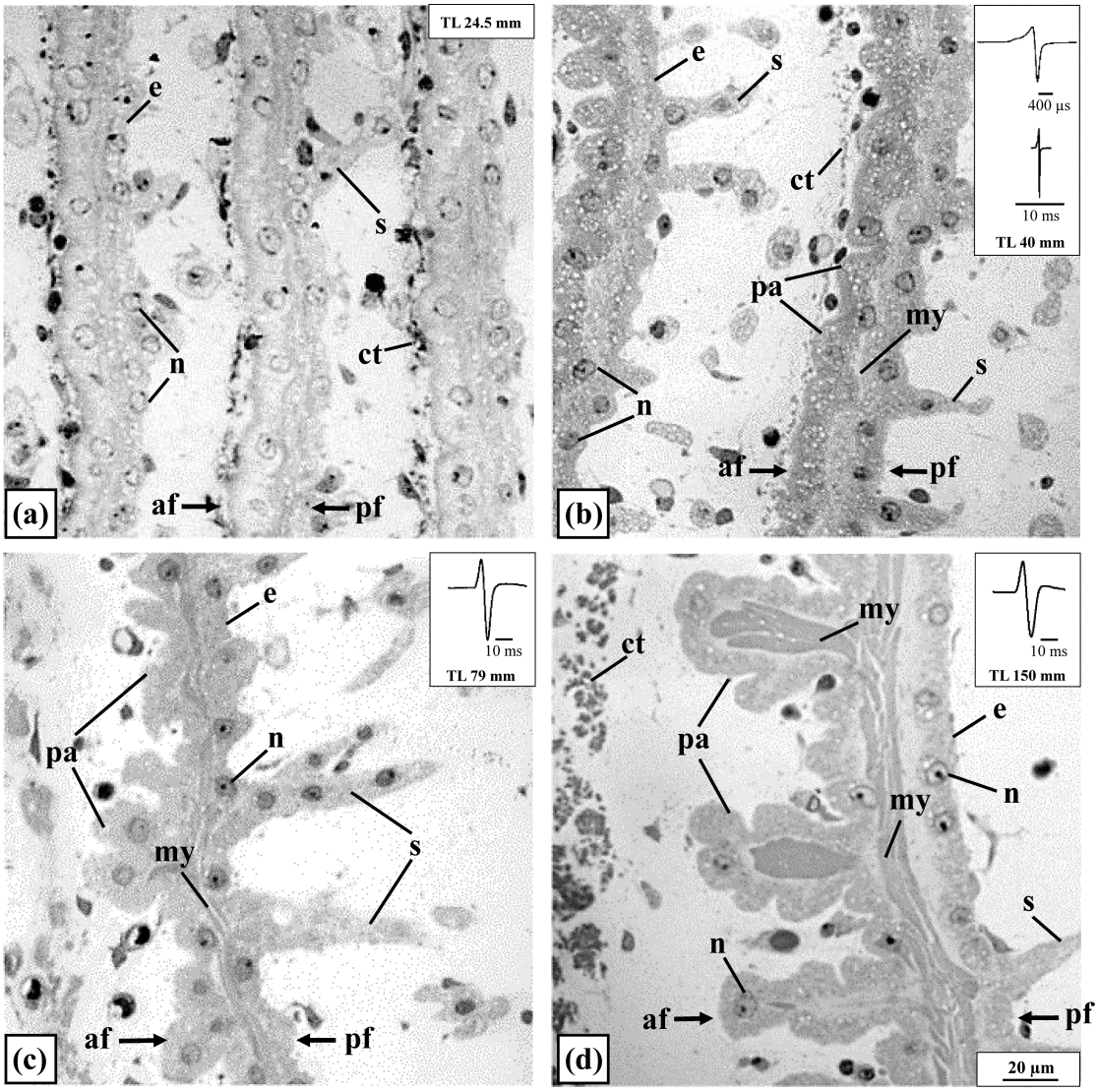

FIGURE 2 Comparison of sagittal semi-thin sections of electrocytes of *Campylomormyrus rhynchophorus* of four developmental stages (a–d); anterior face (af) always to the left. Inserts provide the corresponding EOD and the total length of the fish (TL). Note the absence of papillae (pa) in the smallest fish (a) and the increase in papillae size in the older specimens (b–d). e, electrocytes; ct, connective tissues; s, stalks; n, nuclei; my, myofibrils; af, anterior face; pf, posterior face

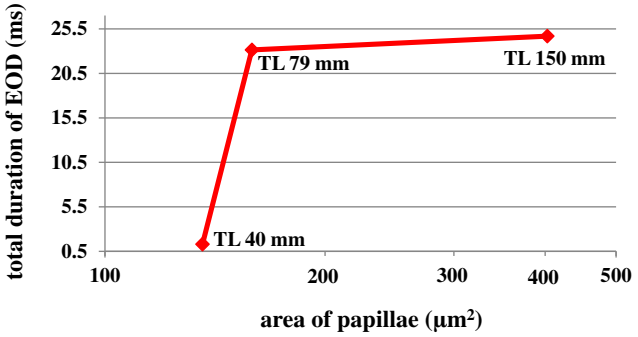

FIGURE 3 Total duration of the EOD and the area of the papillae in three ontogenetic stages of *Campylomormyrus rhynchophorus*. TL, total length of the fish [Color figure can be viewed at wileyonlinelibrary.com]

As shown in Figure 3, there is no linear correlation between EOD duration and papillary size: the large increase in papillary size seen in the largest specimen is not matched by a large increase in EOD duration.

3.4 | Overview of the fine structure of the electrocyte at four developmental stages

In Figure 4, the electrocytes of four developmental stages (24.5 to 150 mm total length) are shown at the electron microscopical level at low magnification. In all stages, centrally located myofibrils are present, whose striation becomes only apparent at higher magnification (see Figures 5 and 7). Furthermore, in addition to cell nuclei, numerous

TABLE 2 Number, length, width, and area (length x width) of the papillae measured in three electrocytes (e) per specimen over a stretch of 200 μm during development

Specimen	Total length of fish mm	Selected electrocyte	No of papillae per 200 μm	Average length of papillae μm	Empirical *SD*	Average width of papillae μm	Empirical *SD* (ESD)	Average area of papillae μm^2	Average area of papillae μm^2 (ESD)
Individual 2	40	1	21	15.44	3.76	10.27	2.67	158.57	135.92 (16.56)
		2	20	12.71	2.37	10.21	2.91	129.77	
		3	19	11.43	2.12	10.45	2.82	119.44	
Individual 3	79	1	17	14.62	3.12	10.76	2.36	157.31	159.82 (17.87)
		2	19	12.78	5.31	10.90	3.15	139.30	
		3	18	16.11	4.73	11.35	3.70	182.85	
Individual 4	150	1	16	24.82	14.38	14.73	6.56	365.60	402.62 (74.74)
		2	14	30.10	14.38	16.84	9.96	506.88	
		3	16	22.77	13.44	14.73	7.12	335.40	

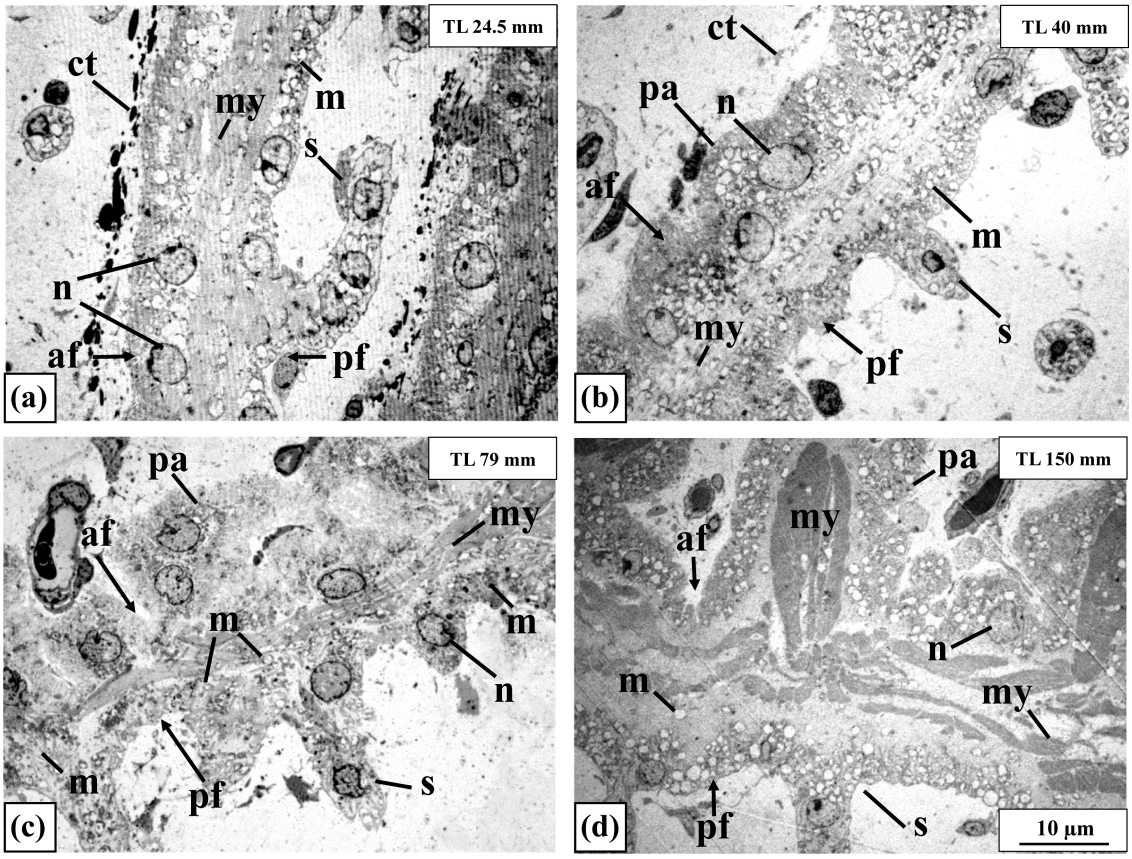

FIGURE 4 Electron micrographs at low magnification of four developmental stages of the electrocytes of *Campylomormyrus rhynchophorus*. Note the absence of papillae (pa) in the youngest stage (a), the beginning of papillae expression in the 40 mm fish (b) and the prominent increase in papillae size at later age (c, d). ct, connective tissues; s, stalks; n, nuclei; my, myofibrils; m, mitochondria; af, anterior face; pf, posterior face

mitochondria are located within both the anterior and posterior face of the electrocytes in all stages with mitochondria being least frequent in the smallest fish. In general, the ultrastructure of the mitochondria is not well preserved. They are swollen and mostly appear as empty round to oval profiles (see also Figures 5, 6, and 8). This could be due to hypoxia during anesthesia (see also DiLisa, Menabo, Canton, & Petronilli, 1998; Herdson, Sommers, & Jennings, 1965) or a consequence of immersion fixation. Stalks, containing nuclei and mitochondria, arise from the posterior face in all stages. The most prominent difference among developmental stages is the organization of the

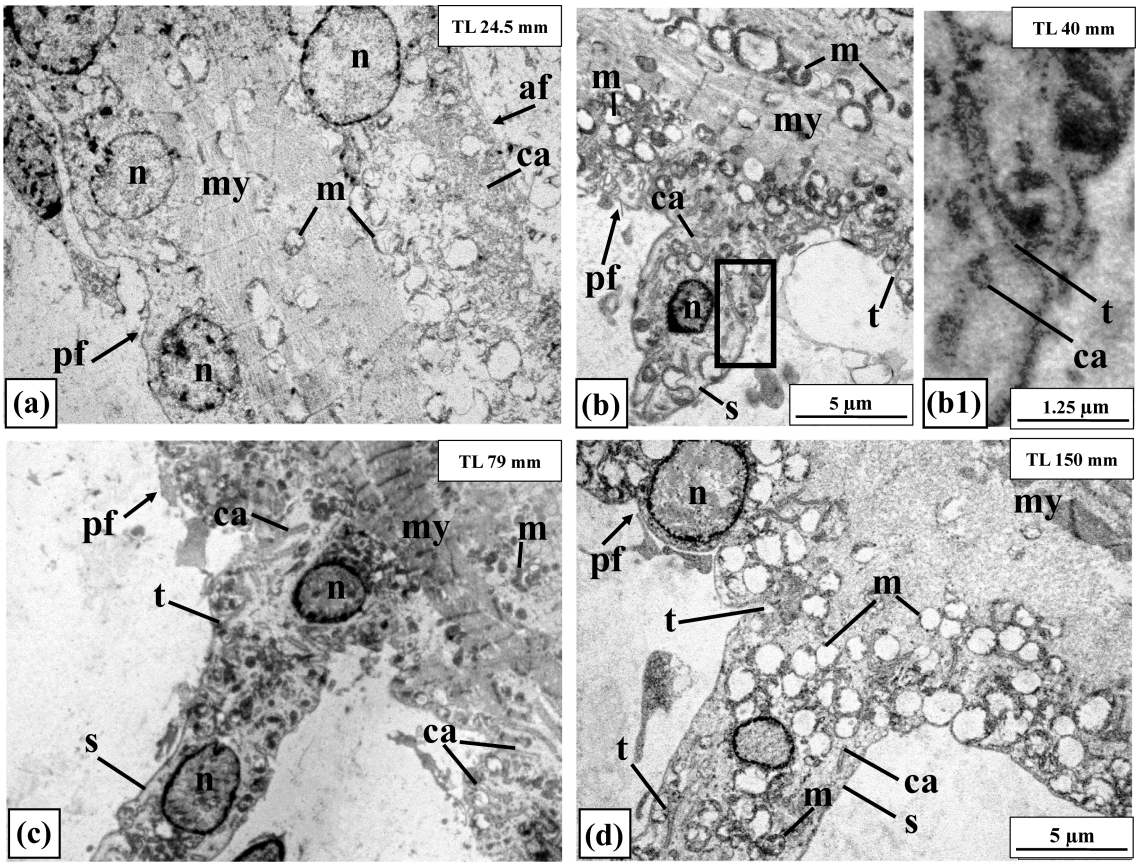

FIGURE 5 Electron micrographs with focus on the posterior face (pf) of the electrocytes in *C. rhynchophorus*. Four developmental stages are shown (a–d). Note the absence of tubules (t) and calveoli (ca) in the posterior face of the smallest specimen. s, stalks; n, nuclei; my, myofibrils; m, mitochondria; af, anterior face; TL, total length of the fish

electrocyte's anterior face: it appears smooth in the 24.5 mm fish (Figure 4a) starts to develop papillae in the 40 mm fish (Figure 4b), and features prominent proliferation of papillae at later stages thereby increasing electrocyte thickness (Figure 4c,d). In the 150 mm fish (Figure 4d), the longest papillae are regularly invaded by myofibrils that extend from the centrally located bundle.

3.5 | Fine structure of the electrocyte's posterior face at four ontogenetic stages

In Figure 5, fine structural features with focus on the posterior face, including the stalks, are shown. Here, the development of surface invaginations, in the form of tubular invaginations (tubules) and calveoli (Bass et al., 1986; Luft, 1958), is of particular interest. These structures are only rarely observed in the material from the smallest specimen (24.5 mm fish, Figure 5a).

In contrast, the posterior face and the stalks of the electrocytes of the next developmental stage (specimen of 40 mm length, Figure 5b) feature tubules and calveoli that are depicted at higher magnification in the insert (Figure 5b11).

The tubules and calveoli remain prominent features in the electrocytes of older specimens (Figure 5c,d).

3.6 | Fine structure of the electrocyte's anterior face at four ontogenetic stages

Papillae are the most prominent structures of the electrocyte's anterior face in mature *C. rhynchophorus*. In Figure 6, we present further details of the ontogeny of the papillae (Figure 6a,c,e,g), and in particular of the ontogeny of the surface invaginations (Figure 6b,d,f,h).

The anterior face of electrocytes in the smallest specimen contains a prominent system of surface invaginations, tubules and calveoli, which contrasts to the posterior face where such specializations develop later (Figures 5a; Figure 6a,b). However, papillae have not yet developed at this stage (see also Figures 2 and 4). In the 40 mm long specimen, round shaped papillae are present that feature numerous tubules and calveoli (Figure 6c,d). The papillae of a 79 mm long specimen have elongated and in a few papillae, the myofibrils extend into the papillae (Figure 6e asterisk). Many calveoli are present, and at the base of the papillae a regular arrangement of calveoli is occasionally seen (Figure 6f).

The longest papillae of the 150 mm long fish typically contain thick bundles of myofibrils (Figures 2d; Figure 4d). Surface specializations include scores of tubules and calveoli (Figure 6g,h).

The density of tubules and calveoli appears lowest in the smallest fish. Further quantification of this parameter and investigations of the

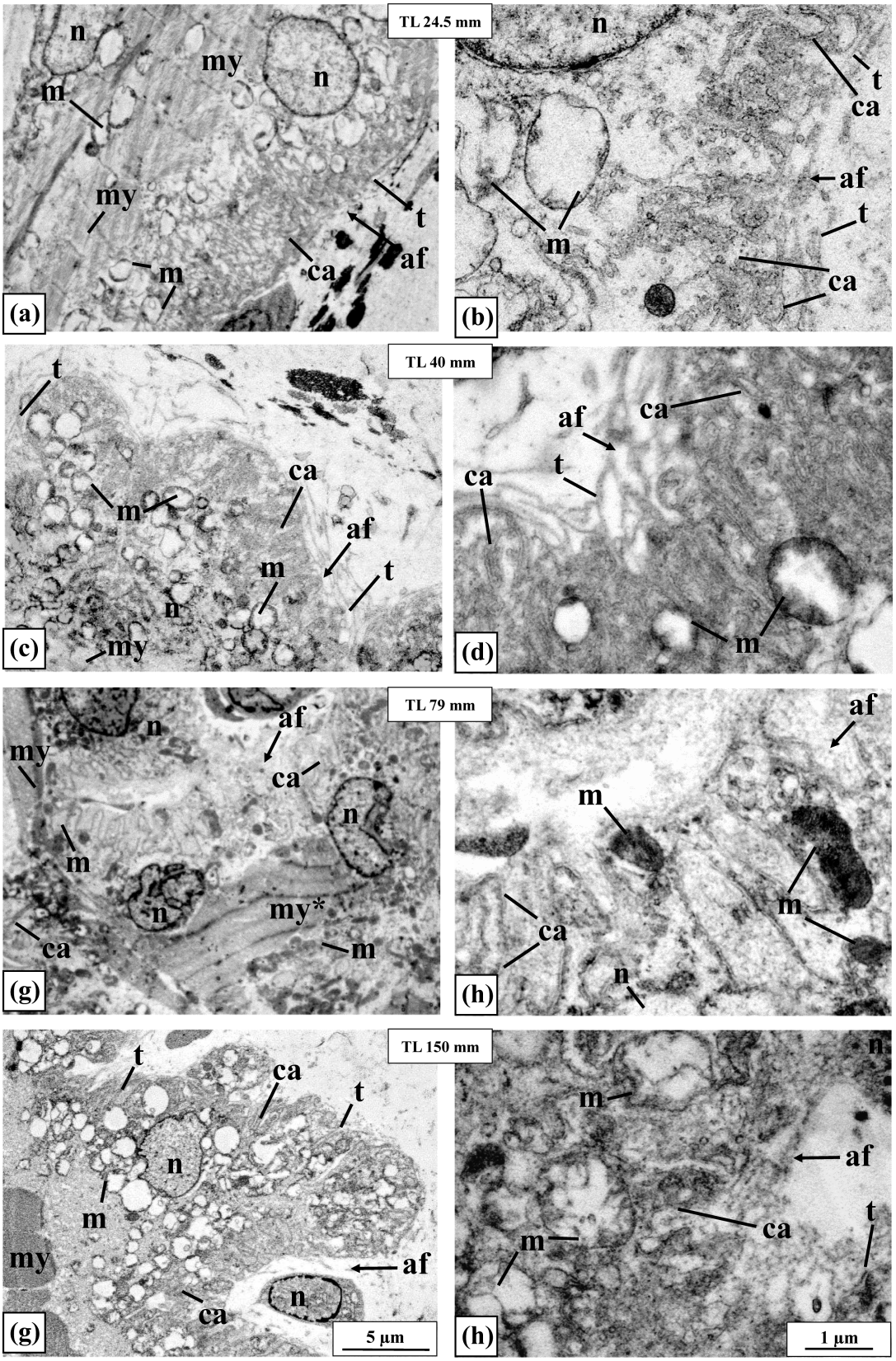

FIGURE 6 Electron micrographs of the anterior face (af) of the electrocyte in *Campylomormyrus rhynchophorus* of four developmental stages. The figures on the left (a, c, e, g) show an overview of the papillae (pa) and those on the right (b, d, f, h) depict relevant details. Asterisk in e indicates myofibrils (my) that enter a papilla. n, nuclei, my (*), myofibrils; m, mitochondria; ca, calveoli; t, tubules; pf, posterior face; TL, total length of the fish

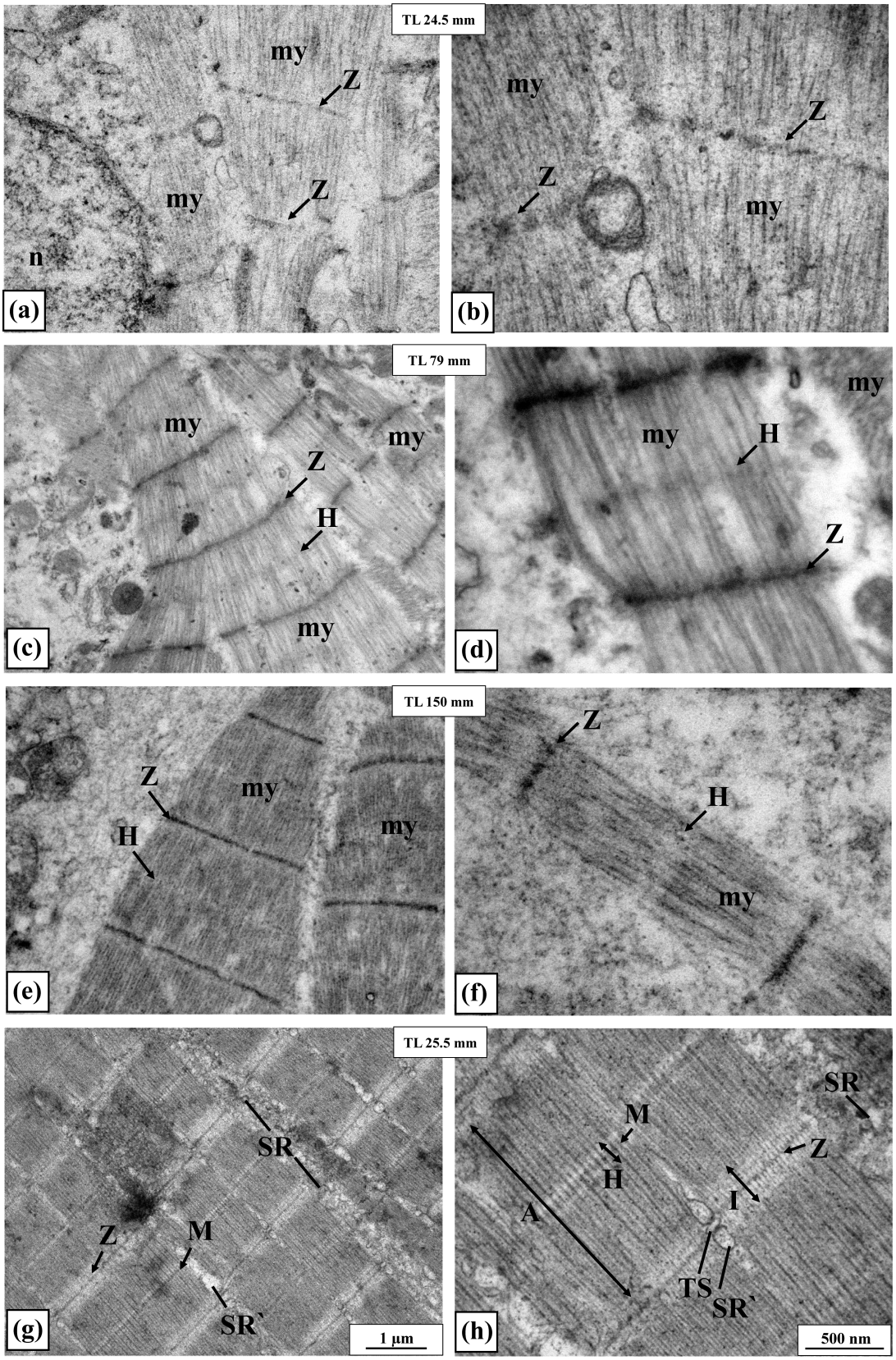

FIGURE 7 Electron micrographs of the myofibrils (my) in the central part of the electrocytes in *Campylomormyrus rhynchophorus* of three developmental stages (a–f). The organization of sarcomeres in skeletal muscle is shown in (g) and (f). my, myofibrils; n, nucleus; Z, Z-lines, H, H-stripe; M, M-lines; SR, endoplasmic reticulum; a, A-zones; I, I-zones; TS, TS-tubule systems; SR′, SR-vesicle systems; TL, total length of the fish

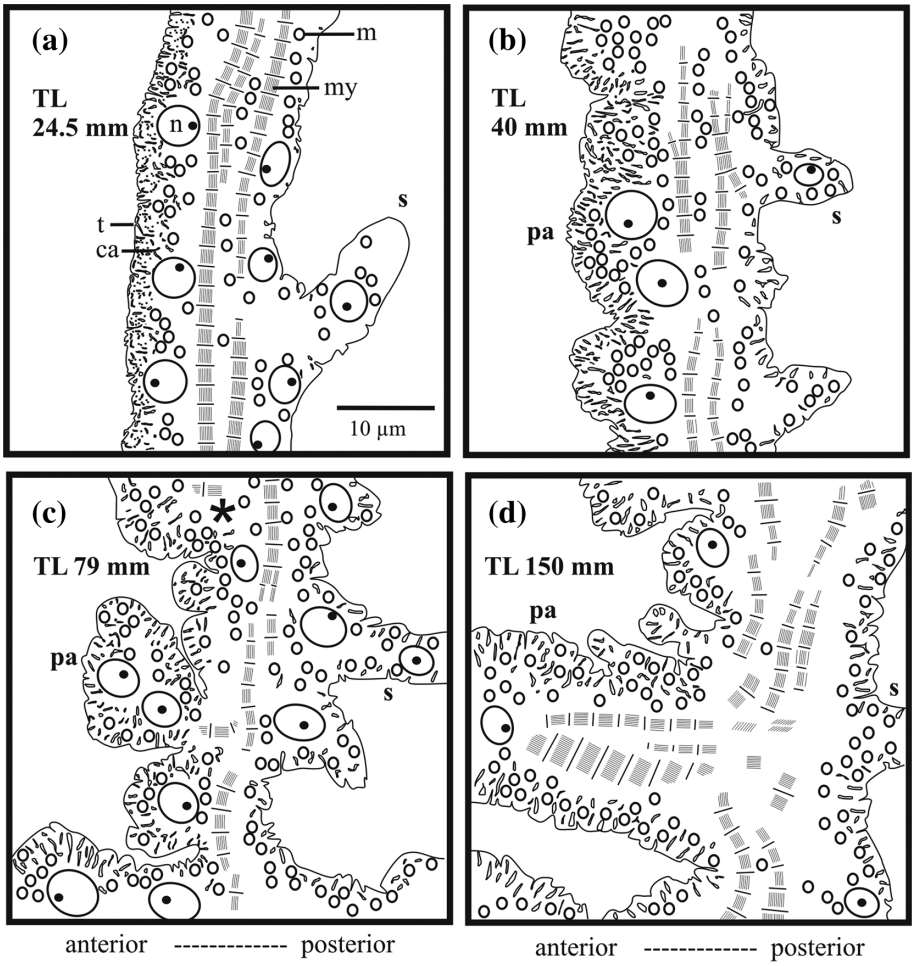

FIGURE 8 Schematic summary drawing of the structural development of the electrocytes in *Campylomormyrus rhynchophorus*. Four developmental stages are shown (a–d). s, stalks; pa, papillae; n, nuclei; my (*), myofibrils; m, mitochondria; ca, calveoli; t, tubules; TL, total length of the fish

length of the tubules, which are thought to arise mostly perpendicular to the electrocyte surface (Bass et al., 1986) is not possible in our material due to the contorted surface of the anterior face and consequently varying cutting angle.

3.7 | Myofibrils in the electrocyte and in the striated muscle

The myofibrils run parallel to the center of the electrocyte in all stages investigated. The bundles, are often, but not regularly, oriented parallel to each other. In addition, numerous mitochondria are arranged near the bundles or in between in all age stages (Figures 4, 5, 8). In the electrocytes of the smallest specimen (total length 24.5 mm), the myofibrils are organized in thick, wide bundles, which sometimes branch into thin layers running parallel to each other (Figures 6a and 7a,b). Z-lines are recognizable and are attached to thin filaments (Figure 7b), but as in older fish, A- and I-zones of the sarcomere, that is, the area between two Z-lines, are not clearly distinct. In fish 79 and 150 mm long, an additional distinct H-stripe occurs in the center of the sarcomere (Figure 7c–f). Myofibrils of the skeletal muscle in the smallest specimen are shown in Figure 7g,h. In contrast to the electrocytes, there is a clear distinction of A- and I-zones, an M-line is present and the TS-tubule and the SR-vesicle systems are well formed (Figure 7g,h).

3.8 | Summary of the ontogenetic change of the fine structure of the electrocytes

The schematic drawing of Figure 8 depicts major structural features of the electrocytes in four developmental stages.

Anterior face: the structural development of the anterior face is dominated by a progressive growth of the papillae with age. Papillae are absent in the youngest stage (24.5 mm long fish, Figures 1a, and 8a) prior to onset of function of the adult EO, start to form as rounded structures in the juvenile fish that produced a short juvenile EOD (40 mm long fish, Figures, asterisk 8b) and further increase in size with age (Figure 8c,d). Tubules and calveoli are present in all developmental stages, and appeared less dense in the youngest fish than at later age. The location of these structures is shown highly simplified in Figure 8a–d. It needs to be emphasized that our material does not provide further information about possible developmental changes in density or dimensions of surface invaginations due to the highly convoluted form of the papillae and thus varying cutting planes. Myofibrils start to invade some papillae in the 79 mm long fish (Figures 6e

and 8c) and regularly occur in the longest papillae of the oldest stage (Figures 2d,8d).

Posterior face: stalks arise from the posterior face of the electrocytes in all developmental stages (Figure 8a–d). Surface invaginations, in the form of tubules and calveoli, were conspicuously absent from the posterior face and stalks of the youngest specimen prior to onset of function. They were well formed at later age always appearing less dense than in the anterior face. Further, quantification of density and dimensions of these structures was not possible in our material.

There is a distinct increase in number of mitochondria with onset of function of the adult EO both in the anterior and posterior faces of the electrocytes (compare Figure 8a,b) likely reflecting the high-energy demands of EOD production (Salazar, Krahe, & Lewis, 2013).

Centrally located myofibrils are present in all developmental stages (Figure 7a–f), whose striation is only schematically indicated in Figure 8.

4 | DISCUSSION

4.1 | Papillae and their impact on the duration of the EOD

The main aim of our study was the investigation of a supposed correlation between the size of the papillae and the duration of the EOD. In mormyrids, the degree of surface area proliferation of the electrocyte, in particular of its anterior face, is positively correlated with EOD duration (Bass et al., 1986). This feature is likely related to an increase in membrane capacitance, which will delay spike initiation (Bass et al., 1986; Bass & Volman, 1987; Bennett, 1970). We examined this possible correlation based on a developmental study in *C. rhynchophorus*.

There was no linear correlation between EOD duration and papillary size, when comparing the three developmental stages of 40, 79, and 150 mm total length (Figure 3). The large increase in duration of the EOD from 1.3 ms (40 mm long fish) to 23.2 ms (79 mm long fish) was accompanied by only a small increase in the size of the papillae (Table 2). In contrast, the large increase in papillary size from the 79 mm fish towards the 150 mm fish was only correlated to a slight increase in EOD duration (23.2 to 24.7 ms). Therefore, the size of the papillae can only to a minor degree be correlated with the duration of the EOD, which is in contrast to the suggestion of, for example, Schwartz, Pappas, and Bennett (1975) and Bass et al. (1986) in studies on weakly electric fish.

Apart from papillary size, the degree of membrane invaginations, such as density and size of tubule-like structures and calveoli, is expected to play a role in shaping EOD duration (Bass et al., 1986). Qualitatively, there was a clear increase in density of these structures both in the anterior and posterior face in the smallest specimen with a functional EO (40 mm long fish) as compared with the earlier stage with a nonfunctional EO (24.5 mm long fish), but differences among the older stages were not obvious in our material. Since we did not perform serial sections and 3D reconstruction, it cannot be excluded that the observed relative small increase (present study) or relative drop in EOD duration (Nguyen et al., 2020) of the largest fish is related to subtle ultrastructural changes of the tubular network such as shorter or fewer tubules.

Additional (physiological) factors, such as a change in gene expression level, might be responsible for the EOD elongation during development. Gallant, Hopkins, and Deitcher (2012) studied gene expression in a mormyrid fish and found 28 genes which were differently expressed when muscle and EO tissues were compared. More specifically, Nagel, Kirschbaum, and Tiedemann (2017) studied voltage gated ion channel genes in *C. compressirostris*, which produces a very short EOD of about 164 μs duration compared with *C. tshokwe* with an EOD of 3.7 ms duration. These authors found an upregulation of all voltage gated ion channel genes in in the EO of *C. tshokwe* compared with that of *C. compressirostris*, but also in *C. tshokwe* when EO and muscle tissue were compared. Neither species develops papillae (Paul et al., 2015) as found in *C. rhynchophorus*. More interestingly, the mormyrid *Gnathonemus petersii* possesses papillae (El Arbani, 2017) but produces only a short EOD of about 250 μs duration (Kirschbaum et al., 2016).

A recent study on gene expression in several *Paramormyrops* operational taxonomic units (Losilla, Luecke, & Gallant, 2020) compared specimens with long and short duration EODs. They did not find evidence of large changes in expression of sodium channels between short duration and long duration species, but they found upregulation in short EOD samples of a voltage sensitive outwardly rectifying potassium channel and of a regulatory subunit of a shall-type voltage-gated potassium channel. The most prominent differences in gene expression between the EOD duration phenotypes comprise genes that code for cytoskeletal, sarcomeric, and lipid metabolism proteins. In a comparable study on gene expression levels between EO and muscle tissue and between the EOs of three mormyrid species (*G. petersii*, *C. compressirostris*, and *C. tshokwe*) Lamanna et al. (2016) conclude that in general terms the most diverging functional classes of genes across the species in the EO include metabolism of fatty acids and ion transport. Although, these investigations are first attempts to understand differences in gene expression between species of different EO characteristics it seems to emerge that each mormyrid genus has followed its own evolutionary pathway to change the duration of the EOD.

4.2 | Papillae in weakly and strongly electric fish

Papillae in weakly electric fish are usually present at the anterior face (Bass, 1986b; Bass et al., 1986; Schwartz et al., 1975). However, there are some exceptions as in *Eigenmannia* sp., where papillae are found at the posterior face of the electrocyte; or they occur on both faces as in *Sternopygus* sp. (Schwartz et al., 1975). In strongly electric fish, papillae either are absent (Luft, 1956) or are found at the innervated posterior or at both, the anterior and posterior faces of the electrocyte (Luft, 1956; Machado, de Souza, Benchimol, Attias, & Porter, 1980; Mermelsstein et al., 1997; Stuart & Kamp, 1934). *Raia*

batis possesses papillae at the posterior face (Stuart & Kamp, 1934). In the little skate *Leucoraja erinacea* papillae are also located at the posterior face (Morson & Morrissey, 2007). In *Electrophorus electricus*, large numbers of fine papillae with minute rodlets are found at both faces. However, the papillae at the anterior face are much larger and thicker than the papillae at the posterior face (Luft, 1956).

The function of the papillae in strongly electric fish is not quite clear (Stuart & Kamp, 1934). Papillae in weakly electric fish are considered to be responsible for the elongation of the EOD duration (Bass et al., 1986; Bennett, 1971; Nguyen et al., 2020; Schwartz et al., 1975); this, however, is in contradiction to the results of this article.

4.3 | Surface invaginations in weakly and strongly electric fish

Increase in surface area is not only obtained by surface evaginations, like papillae, but also by surface invaginations, like tubules and calveoli. They have been described in many species of both weakly and strongly electric fish (Bass, 1986b; Bass et al., 1986; Bennett, 1971; Bruns, 1971; Denizot et al., 1978; Luft, 1956, 1958; Machado et al., 1980; Machado, de Souza, Cotta-Pereira, & Oliveira-Castro, 1976; Mermelsstein et al., 1997; Nguyen et al., 2020; Schwartz et al., 1975; Schwassmann, Assunção, & Kirschbaum, 2014). They are also found at both faces of the electrocyte in *C. rhynchophorus* and increase in density during ontogeny. They increase the surface area of the electrocyte and thus, probably, also contribute to the elongation of the duration of the EOD.

4.4 | The fine structure of the stalk

In mormyrids the stalks, in general, originate at the posterior face of the electrocyte and may, in some species, traverse the electrocyte's body via so called penetrations; in some species the stalks stay on the anterior face (single penetration) or go back to the posterior face (double penetrations) (Bass, 1986b). This geometry is accompanied by different EOD shapes. In *C. rhynchophorus* the stalks arise at the posterior face and do not penetrate the electrocyte. The emerging EOD is a biphasic EOD (Figure 1). During ontogeny, the stalks increase in size, the number of mitochondria increase as well as that of tubules and calveoli (Figure 4). Single nuclei are found in the stalk. A similar fine structure has been described in several *Gnathonemus* species (Bruns, 1971; Schwartz et al., 1975) and in *Pollimyrus isidori* (Denizot et al., 1982). The innervation is found at the tip of the main stalk (Bennett, 1971; Denizot et al., 1982; Szabo, 1958). We have not studied details of the innervation in *C. rhynchophorus*.

4.5 | Myofibrils in the electrocyte and in striated muscle

The central part of the electrocytes of mormyrid fish consists of myofibrils (e.g., Bass, 1986b; Bass et al., 1986; Bruns, 1971; Paul et al., 2015; Schwartz et al., 1975). They are also present in the electrocytes of *C. rhynchophorus*. In contrast to the authors mentioned above, we were able to describe the ontogeny of these myofibrils: they are already found in electrocytes, which are not yet functional (Figure 7a,b). They increase in size and density during ontogeny (Figure 7a–f). We, therefore, believe that these myofibrils are not just remnants of the myogenic origin of the electrocytes (Denizot et al., 1982), instead they are structural elements stabilizing the electrocyte. This view is supported by the fact that the myofibrils extend into the large papillae in the course of ontogeny (Figure 2). This has never been described for the papillae found in other mormyrid fish (Bass, 1986b; Bass et al., 1986; Bruns, 1971; Schwartz et al., 1975), except for *C. numenius* (Paul et al., 2015), the sister species of *C. rhynchophorus* (Lamanna et al., 2016).

The fine structure of the myofibrils of the electrocytes (Figure 7) indicates that they are not functional myofibrils as in striated muscle, because essential elements are missing, such as clear M-lines and the TS-tubule and the SR-vesicle systems (Figure 7a–f).

5 | CONCLUSION

This study explores for the first time the ontogeny of the fine structure of the electrocytes in a mormyrid fish with an EOD of very long duration. It emerges that there is only a very weak correlation between the duration of the EOD and fine structural features like papillae, tubules, and calveoli in contrast to earlier assumptions. The ontogenetic investigation also suggests that the myofibrils which are a remnant of the myogenic origin of the electrocytes serve a structural/stabilizing function. It would be interesting to perform a similar study with the sister species of *C. rhynchophorus*, *C. numenius*, which also produces as adult an EOD of very long duration and possesses papillae.

ACKNOWLEDGMENTS

This study received financial support from the Friedrich Naumann Foundation for Freedom in the course of a scholarship for international PhD students. We would like to thank H. Höft for technical assistance and S. Abelt for the production of the histological preparations and for her support and cooperation during the preparation of semi-thin sections. We thank Prof. Dr. Baumann for the possibility to work in his laboratory during the preparation of semi-thin sections. Thanks go to C. Prietzel and S. Rüstig for their technical support during our investigation on the electron microscope and their interest in our work. We thank Prof. Dr. Krause for his willingness to act as first supervisor of the PhD project of Yevheniia Korniienko. Open access funding enabled and organized by Projekt DEAL.

CONFLICT OF INTEREST

There is no conflict of interest to declare.

AUTHOR CONTRIBUTIONS

Yevheniia Korniienko made substantial contributions to conception and design, acquisition of data, analysis and interpretation of data/

drafted the manuscript/agreed to be accountable for all aspects of the work in ensuring that questions related to the accuracy or integrity of any part of the work are appropriately investigated and resolved/gave final approval of the version to be published. **Ralph Tiedemann** revised the manuscript critically for important intellectual content/gave final approval of the version to be published. **Marianne Vater** made substantial contributions to conception and design, acquisition of data, analysis and interpretation of data/she revised the manuscript critically for important intellectual content/gave final approval of the version to be published. **Frank Kirschbaum** made substantial contributions to conception and design, acquisition of data, analysis and interpretation of data/he revised the manuscript critically for important intellectual content/gave final approval of the version to be published. He agreed to be accountable for all aspects of the work in ensuring that questions related to the accuracy or integrity of any part of the work are appropriately investigated and resolved.

ETHICS APPROVAL

This research was performed in accordance with the German Protection of Animal Act and with Animal Welfare Act and its subsequent amendments. All experiments during this work were conducted with efforts to minimize the number of utilized animals and their suffering.

PEER REVIEW

The peer review history for this article is available at https://publons.com/publon/10.1002/cne.25003.

DATA AVAILABILITY STATEMENT

Data sharing is not applicable to this article as no new data were created or analyzed in this study.

ORCID

Frank Kirschbaum https://orcid.org/0000-0002-3046-5218

REFERENCES

Bass, A. H. (1986a). Electric organs revisited: Evolution of a vertebrate communication and orientation organ. In T. H. Bullock & W. Heiligenberg (Eds.), *Electroreception*. New York: Wiley.

Bass, A. H. (1986b). Species differences in electric organs of mormyrids: Substrates for species-typical electric organ discharge waveforms. *The Journal of Comparative Neurology*, *244*, 313–330.

Bass, A. H., Denizot, J. P., & Marchaterre, M. A. (1986). Ultrastructural features and hormone dependent sex differences of mormyrid electric organs. *The Journal of Comparative Neurology*, *254*, 511–528.

Bass, A. H., & Volman, S. F. (1987). From behavior to membranes: Testosterone-induced changes in action potential duration in electric organs. *Proceedings of the National Academy of Sciences of the United States of America*, *84*, 9295–9298.

Bennett, M. V. L. (1970). Comparative physiology: Electric organs. *Annual Review of Physiology*, *32*, 471–528. https://doi.org/10.1146/annurev.ph.32.030170.002351

Bennett, M. V. L. (1971). Electric organs. In W. S. Hoar & D. J. Randall (Eds.), *Fish physiology*. New York: Academic Press.

Bennett, M. V. L., & Grundfest, H. (1961). Studies on morphology and electrophysiology of electric organs. III electrophysiology of electric organs in mormyrids. In C. Chagas & A. Paes de Carvalho (Eds.), *Bioelectrogenesis*. London, New York, Princeton: Elsevier Publishing Company.

Bruns, V. (1971). Elektrisches Organ von *Gnathonemus* (Mormyridae). *Zeitschrift für Zellforschung und Mikroskopische Anatomie*, *122*, 538–563.

Bullock, T. H., & Heiligenberg, W. (1986). *Electroreception*. New York: John Wiley & Sons.

Bullock, T. H., Hopkins, C. D., Popper, A. N., & Fay, R. R. (2005). *Electroreception*. New York: Springer.

Crampton, W. G. R. (2006). Evolution of electric signal diversity in gymnotiform fishes II. Signal design. In F. Ladich, S. P. Collin, P. Moller, & B. G. Kapoor (Eds.), *Communication in fishes*. Enfield, NH: Science Publishers.

Crampton, W. G. R., Rodriguez-Cuttaneo, A., Lovejoy, N. R., & Caputi, A. A. (2013). Proximate and ultimate causes of signal diversity in the electric fish *Gymnotus*. *The Journal of Experimental Biology*, *216*, 2523–2541.

Denizot, J. P., Kirschbaum, F., Westby, G. W. M., & Tsuji, S. (1978). The larval electric organ of the weakly electric fish *Pollimyrus* (*Marcusenius*) *isidori* (Mormyridae, Teleostei). *Journal of Neurocytology*, *7*, 165–181.

Denizot, J. P., Kirschbaum, F., Westby, G. W. M., & Tsuji, S. (1982). On the development of the adult electric organ in the mormyrid fish *Pollimyrus isidori* (with special focus on the innervation). *Journal of Neurocytology*, *11*, 913–934.

DiLisa, F., Menabo, R., Canton, M., & Petronilli, V. (1998). The role of mitochondria in the salvage and the injury of the ischemic myocardium. *Biochimica et Biophysica Acta*, *1366*(1–2), 69–78.

El Arbani, K. (2017). *Ontogeny of morphology, electric organ and electric organ discharge of intra- and intergenus hybrids in the weakly electric fish Campylomormyrus and Gnathonemus (Mormyridae)*. (Master thesis), Humboldt University of Berlin, Germany.

Feulner, P. G. D., Kirschbaum, F., Mamonekene, V., Ketmaier, V., & Tiedemann, R. (2007). Adaptive radiation in African weakly electric fish (Teleostei: Mormyridae: *Campylomormyrus*): A combined molecular and morphological approach. *Journal of Evolutionary Biology*, *20*, 403–414.

Feulner, P. G. D., Kirschbaum, F., & Tiedemann, R. (2008). Adaptive radiation in the Congo River: An ecological speciation scenario for African weakly electric fish (Teleostei; Mormyridae; *Campylomormyrus*). *Journal of Physiology, Paris*, *102*, 340–346.

Gallant, J. R., Hopkins, C. D., & Deitcher, D. L. (2012). Differential expression of genes and proteins between electric organ and skeletal muscle in the mormyrid electric fish *Brienomyrus brachyistius*. *The Journal of Experimental Biology*, *215*, 2479–2494. https://doi.org/10.1242/jeb.063222

Herdson, P. B., Sommers, H. M., & Jennings, R. B. (1965). A comparative study of the fine structure of normal and ischemic dog myocardium with special reference to early changes following temporal occlusion of a coronary artery. *The American Journal of Pathology*, *46*, 367–386.

Kirschbaum, F. (1977). Electric-organ ontogeny - distinct larval organ precedes adult organ in weakly electric fish. *The Science of Nature*, *64*, 387–388. https://doi.org/10.1007/BF00368748

Kirschbaum, F. (1981). Ontogeny of both larval electric organ and electromotoneurones in *Pollimyrus isidori* (Mormyridae, Teleostei). In T. Szabo & G. Czeh (Eds.), *Advances in physiological sciences, sensory physiology of aquatic lower vertebrates*. Budapest: Pergamon Press.

Kirschbaum, F. (2020). Structure and function of electric organs. In F. Kirschbaum & K. Formicki (Eds.), *The histology of fishes*. Boca Raton: CRC Press, Taylor and Francis Group.

Kirschbaum, F., Nguyen, L., Baumgartner, S., Chi, L., Wolfart, R., Elarbani, K., … Vater, M. (2016). Intragenus (*Campylomormyrus*) and intergenus hybrids in mormyrid fish: Physiological and histological investigations of the electric organ ontogeny. *Journal of Physiology, Paris*, *110*, 281–301. https://doi.org/10.1016/j.jphysparis.2017.01.003

Kramer, B. (1990). *Electrocommunication in teleost fishes: Behavior and experiments*. Berlin: Springer.

Lamanna, F., Kirschbaum, F., & Tiedemann, R. (2016). Species delimitation and phylogenetic relationships in a genus of African weakly electric fish (Osteoglossiformes, Mormyridae, *Campylomormyrus*). *Molecular Phylogenetics and Evolution*, *101*, 8–18.

Losilla, M., Luecke, D. M., & Gallant, J. R. (2020). The transcriptional correlates of divergent electric organ discharges in *Paramormyrops* electric fish. *BMC Evolutionary Biology*, *20*(1), 1–19. https://doi.org/10.1186/s12862-019-1572-3

Luft, J. H. (1956). The fine structure of the electric organ of the electric eel and torpedo ray. *The Journal of Biophysical and Biochemical Cytology*, *2*(4), 229–232.

Luft, J. H. (1958). The fine structure of electric tissues. *Experimental Cell Research. Supplement*, *5*, 168–182.

Machado, R. D., de Souza, W., Benchimol, M., Attias, M., & Porter, K. R. (1980). Observations on the innervated face of the electrocyte of the main organ of the electric eel (*Electrophorus electricus* L.). *Cell and Tissue Research*, *213*, 69–80.

Machado, R. D., de Souza, W., Cotta-Pereira, G., & Oliveira-Castro, G. (1976). On the fine structure of the electrocyte of *Electrophorus electrieus* L. *Cell and Tissue Research*, *174*, 355–366.

Mermelsstein, C. d. S., Benchimol, M., Taffarel, M., Cordeiro, M. C. R., Chagas, C., & Neto, V. M. (1997). Desmin and Actin filaments in membrane-cytoskeletal preparations of the electric tissue of *Electrophorus electricus* L. *Archives of Histology and Cytology*, *60*(5), 445–452.

Moller, P. (1995). *Electric fishes: History and behavior*. London: Chapman and Hall.

Morson, J. M., & Morrissey, J. F. (2007). Morphological variation in the electric organ of the little skate (*Leucoraja erinacea*) and its possible role in communication during courtship. *Environmental Biology of Fishes*, *80*, 267–275.

Nagel, R., Kirschbaum, F., & Tiedemann, R. (2017). Electric organ discharge diversification in mormyrid weakly electric fish is associated with differential expression of voltage-gated ion channel genes. *Journal of Comparative Physiology. A*, *203*, 183–195. https://doi.org/10.1007/s00359-017-1151-2

Nguyen, M. D. L., Mamonekene, V., Vater, M., Bartsch, P., Tiedemann, R., & Kirschbaum, F. (2020). Ontogeny of electric organ and electric organ discharge in *Campylomormyrus rhynchophorus* (Teleostei: Mormyridae). *Journal of Comparative Physiology. A*, *206*, 453–466. https://doi.org/10.1007/s00359-020-01411-z

Nguyen, M. D. L., Paul, C., Mamonekene, V., Bartsch, P., Tiedemann, R., & Kirschbaum, F. (2017). Reproduction and development in some species of the weakly electric genus *Campylomormyrus* (Mormyridae, Teleostei). *Environmental Biology of Fishes*, *100*(1), 49–68. https://doi.org/10.1007/s10641-016-0554-1

Paul, C., Mamonekene, V., Vater, M., Feulner, P. G., Engelmann, J., Tiedemann, R., & Kirschbaum, F. (2015). Comparative histology of the adult electric organ among four species of the genus *Campylomormyrus* (Teleostei: Mormyridae). *Journal of Comparative Physiology. A*, *201*, 357–374.

Robinson, D. G., Ehlers, U., Herken, R., Herrmann, B., Mayer, F., & Schürmann, F.-W. (1985). *Präparationsmethodik in der Elektronenmikroskopie: Eine Einführung für Biologen und Mediziner*. Berlin, Heidelberg, New York, Tokyo: Springer-Verlag Berlin Heidelberg GmbH.

Salazar, V. L., Krahe, R., & Lewis, J. E. (2013). The energetics of electric organ discharge generation in gymnotiform weakly electric fish. *The Journal of Experimental Biology*, *216*, 2459–2468.

Schwartz, I. R., Pappas, G. D., & Bennett, M. . V. L. (1975). The fine structure of electrocytes in weakly electric teleosts. *Journal of Neurocytology*, *4*, 87–114.

Schwassmann, H. O., Assunção, M. I., & Kirschbaum, F. (2014). Ontogeny of the electric organs in the electric eel, *Electrophorus electricus*: physiological, histological, and fine structural investigations. *Brain, Behavior and Evolution*, *84*(4), 288–302.

Stuart, C., & Kamp, C. J. (1934). The electric organ and its centres in *Torpedo marmorata*. *Proceedings van de Koninklijke Nederlandse Akademie van Wetenschappen*, *37*, 342–347.

Sullivan, J. P., Lavoué, S., & Hopkins, C. D. (2016). *Cryptomyrus*: A new genus of Mormyridae (Teleostei, Osteoglossomorpha) with two new species from Gabon, West-Central Africa. *Zookeys*, *561*, 117–150. https://doi.org/10.3897/zookeys.561.7137

Szabo, T. (1958). Structure intime de l'organe electrique de trois mormyrides. *Zeitschrift für Zellforschung und Mikroskopische Anatomie*, *49*, 33–45. https://doi.org/10.1007/BF00335061

Szabo, T. (1960). Development of the electric organ of Mormyridae. *Nature*, *188*, 760–762.

Szabo, T. (1974). Anatomy of the specialized lateral line organs of electroreception. In A. Fessard (Ed.), *Electroreceptors and other specialized receptors in lower vertebrates*. Berlin, Heidelberg, New York: Springer Verlag.

von der Emde, G. (1992). Electrolocation of capacitive objects in four species of pulse-type weakly electric fish: II. Electric signalling behaviour. *Journal of Ethology*, *92*, 177–192.

von der Emde, G. (1999). Active electrolocation of objects in weakly electric fish. *The Journal of Experimental Biology*, *202*, 1205–1215.

von der Emde, G. (2006). Non-visual environmental imaging and object detection through active electrolocation in weakly electric fish. *Journal of Comparative Physiology*, *192*(6), 601–612.

Webb, F. W., Collin, S. P., Kuciel, M., Schulz-Mirbach, T., Zuwala, K., Denizot, J. P., & Kirschbaum, F. (2020). Sensory organs. In F. Kirschbaum & K. Formicki (Eds.), *The histology of fishes*. Boca Raton: CRC Press, Taylor and Francis Group.

Werneyer, M., & Kramer, B. (2006). Ontogenetic development of electric-organ discharges in a mormyrid fish, the bulldog *Marcusenius macrolepidotus* (south African form). *Journal of Fish Biology*, *69*(4), 1190–1201. https://doi.org/10.1111/j.1095-8649.2006.01195

Westby, G. M., & Kirschbaum, F. (1977). Emergence and development of the electric organ discharge in the mormyrid fish, *Pollimyrus isidori*. I. The larval discharge. *Journal of Comparative Physiology*, *122*, 251–271.

Westby, G. M., & Kirschbaum, F. (1978). Emergence and development of the electric organ discharge in the mormyrid fish, *Pollimyrus isidori*. II. Replacement of the larval by the adult discharge. *Journal of Comparative Physiology*, *127*, 45–59.

Worm, M. F., Kirschbaum, F.,& von der Emde, G. (2017). Social interactions between live and artificial weakly electric fish: Electrocommunication and locomotor behavior of *Mormyrus rume proboscirostris* towards a mobile dummy fish. PLoS One, 12(9). https://doi.org/10.1371/journal.pone.0184622

How to cite this article: Korniienko Y, Tiedemann R, Vater M, Kirschbaum F. Ontogeny of the electric organ discharge and of the papillae of the electrocytes in the weakly electric fish *Campylomormyrus rhynchophorus* (Teleostei: Mormyridae). *J Comp Neurol*. 2021;529:1052–1065. https://doi.org/10.1002/cne.25003